Multiple-Site Optical Recording of Membrane Potential from a Salivary Gland

Interaction of Synaptic and Electrotonic Excitation

D. M. SENSEMAN, H. SHIMIZU, I. S. HORWITZ, and B. M. SALZBERG

From the Department of Physiology and Pharmacology, School of Dental Medicine, and the Institute of Neurological Sciences, University of Pennsylvania, Philadelphia, Pennsylvania 19104

ABSTRACT The interaction between synaptic and electrotonic excitation of cells from the salivary gland of the snail *Helisoma trivolvis* was studied using a voltage-sensitive merocyanine dye. Linear and square photodiode matrix arrays were used to record simultaneously the response to neuronal stimulation of 15–25 separate regions of the gland. Laterally opposed acini exhibited highly synchronous electrical activity, which suggested a correspondingly high degree of electrical coupling. In the longitudinal direction, coupling appeared weaker. The onset of depolarization after neuronal stimulation was progressively delayed along the longitudinal gland axis, in agreement with the measured conduction velocity of the presynaptic nerve spike. In most instances, neuronal stimulation directly activated a regenerative gland response (action potential) at the junction between the anterior and central duct. Excitation of distal gland regions was usually mediated by electrotonic spread from active, more proximal gland regions. Occasionally, "collisions" between excitatory waves traveling in opposite directions were observed.

INTRODUCTION

Electrical coupling between adjacent secretory acinar cells has been demonstrated in a number of exocrine gland tissues derived from both invertebrate and vertebrate species (e.g., Simpson et al., 1977; Ginsborg et al., 1974; Petersen and Ueda, 1976; Iwatsuki and Petersen, 1978*a*, *b*; Roberts et al., 1978; Kater and Galvin, 1978). Although electrical coupling appears to be a general characteristic of exocrine (and endocrine) glands, its functional significance is still unclear (Petersen, 1980). It has been suggested that in glands that receive direct neural innervation, such as mammalian salivary glands, the syncytial character of the tissue may play an important role in the

Address reprint requests to Dr. D. M. Senseman, Dept. of Physiology, University of Pennsylvania, School of Dental Medicine, 4001 Spruce St., Philadelphia, PA 19104. Dr. Shimizu's current address is Optoelectronics Section, Electrotechnical Laboratory, 1-1-4, Umezono, Sakura-mura, Ibaraki 305, Japan.

J. GEN. PHYSIOL. © The Rockefeller University Press · 0022-1295/83/06/0887/22 $1.00 887
Volume 81 June 1983 887–908

excitation process. Since electrical coupling would permit a sudden change in membrane potential initiated at one gland locus to spread rapidly to adjacent regions, acinar cells receiving direct neural innervation could communicate an excitatory input to surrounding noninnervated acinar cells (Young and van Lennep, 1978).

To examine the interaction between direct synaptic depolarization and electronic spread from synaptically activated gland regions, we studied a relatively simple salivary gland system from the snail *Helisoma trivolvis*. It has been shown that the snail salivary gland receives a direct excitatory input from a bilateral pair of identifiable neurons located in the buccal ganglia, and there is some evidence to suggest that only a specific subpopulation of acinar secretory cells receive a direct synaptic input since significant regional differences have been observed in the numbers of acinar cells exhibiting "fast-rise-time" miniature potentials (Kater et al., 1978*a*, *b*; Bahls et al., 1980). Acinar cells in the snail differ from their mammalian counterparts, however, in at least one important respect. Although neural stimulation leads to a relatively slow, predominantly hyperpolarizing response in mammalian acinar cells (e.g., Lundberg, 1955; Kagayama and Nishiyama, 1974), snail acinar cells exhibit a transient depolarization similar in size and waveform to a conventional excitatory postsynaptic potential (EPSP) (Kater et al., 1978*b*; Bahls et al., 1980). Frequently, this transient depolarization is followed by the appearance of an overshooting action potential in the acinar cell ("gland spike"). Electrical coupling then permits action potentials initiated at one gland locus to activate adjacent regions and a regenerative response is propagated throughout the gland (Kater et al., 1978*a*). Thus, intercellular electrotonic coupling provides a secondary source of depolarization in the excitatory process, after the initial transient depolarization produced by the neural input (i.e., the EPSP).

The relative importance of synaptic compared with electrotonic depolarization will depend upon a number of factors, including the efficacy and distribution of excitatory synaptic inputs as well as the cable properties of the syncytium. If synaptic efficacy is low or the distribution of synapses is spatially restricted, activation of the entire gland after action potentials in the salivary effector neurons (SENs) will require extensive electrotonic spread. Conversely, if synaptic efficacy is high, and excitatory synaptic inputs are uniformly distributed throughout the gland, then the contribution of electrotonic spread to the excitation process will be less significant. To investigate the interaction of synaptic and electrotonic excitation in the snail salivary gland, we have used a potentiometric probe (for reviews see Cohen and Salzberg, 1978; Waggoner, 1979; Salzberg, 1983) together with a multiple-site optical recording system (Salzberg et al., 1977; Grinvald et al., 1981) to monitor changes in membrane potential simultaneously in 15–25 different gland regions. We have found that excitatory synaptic inputs appear to be uniformly distributed along the entire gland surface so that neural stimulation leads to a transient depolarization of the entire gland. However, although this depolarization generally initiates action potentials locally in one or more gland regions, it does not directly activate the entire gland. Instead, complete activation is

achieved by the electrotonic propagation of the action potential from the active regions. Preliminary reports of this work have been published (Salzberg and Senseman, 1979; Senseman and Salzberg, 1980; Salzberg et al., 1981).

METHODS

Preparation

Salivary glands were obtained from an inbred line (Red 1) of the basommatophoran snail, *Helisoma trivolvis*, derived from breeding stock kindly provided by Dr. S. B. Kater, University of Iowa, Iowa City, IA. Glands were surgically removed from adult specimens (shell diameters 1.2–1.7 cm) as previously described by Kater et al. (1978*a*). In most animals (>80%), the bilaterally paired salivary glands were fused at their aboral terminations, forming a single tubular structure, whereas in the remaining specimens, the left and right salivary glands were anatomically distinct. Both fused and nonfused glands were used in the experiments described below. In some experiments, the buccal ganglia were left attached to a gland by the salivary gland nerve, which enters the ganglia via the esophageal trunk. Miniature staples, fashioned from 50-μm-diam tungsten wire, were used to secure the preparation to a thin layer of clear Sylgard resin, which formed the bottom of a simple chamber mounted on the stage of a compound microscope.

Electrophysiological Methods

Conventional intracellular microelectrode recording techniques were used to monitor electrical activity in single salivary gland acinar cells and/or in the bilaterally paired SENs. Glass-fiber micropipettes filled with 2.5 M KCl (10–30 MΩ) were connected by means of a Ag/AgCl wire to a commercially available intracellular preamplifier equipped with an active bridge circuit for current injection (Neuroprobe model 1600; Transidyne General, Ann Arbor, MI). The output of the preamplifier was monitored on an oscilloscope and passed to a high-speed analog-to-digital converter for storage and subsequent analysis (see below).

For preparations in which the salivary gland nerve was stimulated directly, the cut end of the nerve was drawn into a suction electrode fabricated from Tygon tubing, which had been hand-pulled to a fine tip over a low-temperature flame.

Optical Recording Methods

Procedures for optical monitoring of membrane potential in isolated snail salivary glands have been reported previously (Senseman and Salzberg, 1980). The preparation chamber was mounted on the stage of a Reichert Zetopan compound microscope (American Optical Co., Buffalo, NY), modified to permit coarse and fine focusing of the tube head with the stage fixed. Bright field illumination was provided by a 100-W quartz-halogen tungsten-filament lamp driven by a stable DC power supply (model JQE 75-15; Kepco Inc., Flushing, NY). Incident light was collimated, passed through a KG1 heat filter (Schott Optical Glass Inc., Duryea, PA), rendered quasi-monochromatic with a 675-nm (± 26 nm full width at half maximum) interference filter, and focused onto the preparation by means of a large-aperture substage condenser. A long working distance objective collected light transmitted by the preparation and formed a real image on a photodiode array located in the objective image plane. Magnifications varied from 3.2 to 20 in different experiments. Vibrational noise arising at the air/water interface was eliminated either by using water-immersion objectives (i.e.,

× 10 and 20) or by covering the central region of the chamber with a microscope slide coverslip.

Two silicon photodiode arrays were used interchangeably to measure the light intensity passing through various regions of the gland. A 5- × 5-element square array (model MD-25-0; Integrated Photomatrix Ltd./Centronics, Mountainside, NJ) provided two-dimensional information on membrane potential changes in the gland, and a 20-element linear array (model LD-20-5; IPL/Centronics) permitted improved spatial resolution along a single axis. In the image plane of the microscope, the gland was viewed on a fine ground-glass screen bearing an accurately scribed replica of either array. The preparation was positioned on the image of the array, and a drawing was prepared of the gland superimposed on the photodiode matrix. This map was later used to correlate changes in membrane potential with particular anatomical locations on the gland.

The photocurrents generated by each array element were separately converted to voltages and amplified as described previously (Salzberg et al., 1977; Grinvald et al., 1981), except that we extended the low-frequency time constant of the capacity-coupled recording system to 1.0 s in order to minimize the AC distortion introduced into the recording of the relatively slow potential changes in this preparation. The low-pass filter was adjusted to give a response time of 1.1 ms (10–90% final amplitude). In some experiments, selected outputs of the current-to-voltage amplifiers were passed in parallel to a 16-channel computer-based signal analyzer (model TN 1500; Tracor-Northern Inc., Middleton, WI) and the digitized signals were stored on magnetic tape for display and analysis. However, in most experiments, all amplifier outputs were fed into a computer-based, 128-channel data-acquisition system capable of acquiring a complete frame every 0.8 ms, similar to that described recently by Grinvald et al. (1981). Software for data acquisition and display was generously provided by Larry Cohen and Sarah Lesher, Yale Medical School, New Haven, CT. Vibrational noise in the system was reduced by means of a large vibration isolation table (Newport Research Inc., Fountain Valley, CA).

Staining Procedure

Salivary glands were surgically removed and mounted in the recording chamber in normal snail Ringer's solution having the following composition (mM): 51.3 NaCl; 1.7 KCl; 4.1 $CaCl_2$; 1.5 $MgCl_2$; and 1.8 $NaHCO_3$; adjusted to pH 7.5. Before staining, the preparation was superfused with a Ringer's solution having the same ionic composition, except that the $CaCl_2$ and $MgCl_2$ concentrations were raised to 20 mM (replacing NaCl), which had the effect of reducing or eliminating dye-related pharmacological effects (Salzberg et al., 1981). After a 2–5 min exposure to the high-divalent cation Ringer's, the preparation was stained for 20–50 min with 0.05 mg/ml of a merocyanine-oxazolone dye, NK 2367 (Nippon Kankoh-Shikiso Kenkyusho Co., Okayama, Japan) dissolved in the high-divalent cation ringer. (Although longer staining times provided larger optical signals, the probability of pharmacological effects was increased.) The preparation was then washed with the high-divalent cation Ringer's, followed by a 3-min exposure to normal snail Ringer's containing 10 mM sodium metavanadate (81103; Alfa Products, Danvers, MA) to block ciliary activity (Salama et al., 1980). The preparation was washed with several changes of normal snail Ringer's and allowed to stabilize for a period of not less than 5 min before the first experimental trial. To minimize dye bleaching after the staining period, a low level of blue light (<480 nm) was used to illuminate the optical field during the insertion of microelectrodes.

RESULTS

Inhibition of Ciliary Beating

Transport of secretory products through the snail salivary gland is accomplished in part by the metachronous beating of cilia lining the luminal gland surface (Kater et al., 1978*a*). This ciliary activity proved to be an important source of optical noise in our early attempts to monitor electrical activity using a photodiode array (Fig. 1). To improve the signal-to-noise ratio for the

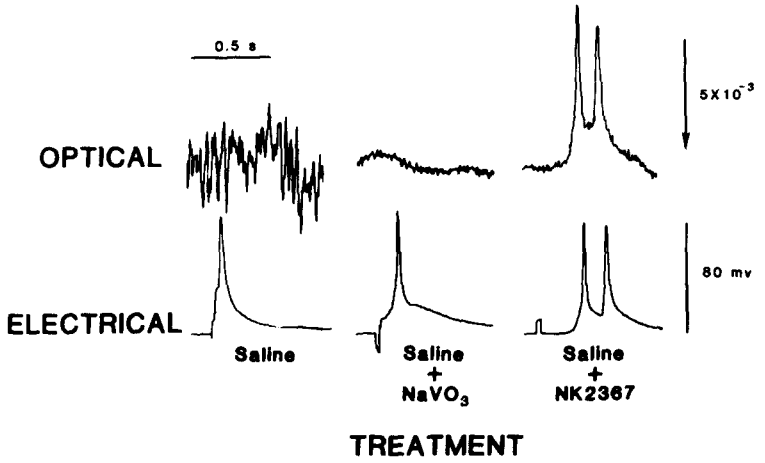

FIGURE 1. Reduction of cilia-induced optical noise by sodium metavanadate ($NaVO_3$) treatment. The lower trace (electrical) is an intracellular recording from an acinar gland cell; the upper trace (optical) is the amplified AC-coupled output of a single photodetector element of the photodiode array monitoring light transmitted through a gland region near the site of microelectrode impalement. In this and in all subsequent figures, the arrow points in the direction of increasing light intensity, while its length indicates the size of the optical change relative to the resting light level. The pair of traces on the left were obtained from the unstained preparation bathed in normal saline. The central pair of traces show the effect on the optical noise level of exposing the unstained preparation to saline containing 10 mM $NaVO_3$ for 6 min. The pair of traces on the right show the effect of staining the same preparation with 50 μg/ml of NK2367 for 20 min after vanadate treatment. Changes in transmitted light corresponding to membrane potential changes were observable only after staining. In each of the three trials, a brief shock was delivered to the cut salivary nerve to stimulate the gland.

extrinsic absorption signal, it was necessary to identify an inhibitor of ciliary motility. A substantial reduction in cilia-induced noise was achieved by exposing the gland to a normal Ringer's solution containing 10 mM sodium metavanadate ($NaVO_3$) for 3–6 min (Fig. 1). After washout of the $NaVO_3$, ciliary activity remained suppressed for ~1 h, after which some recovery in function was usually observed.

Sodium metavanadate has been shown to alter a number of cellular processes (e.g., Westenfelder et al., 1981; Křivánek, 1981) in addition to its inhibitory effect on ciliary motility (Gibbons et al., 1978). In the snail salivary gland preparation, control experiments using conventional intracellular microelectrodes demonstrated that prolonged exposure to 10 mM $NaVO_3$ (>20 min) had little effect on either the resting membrane potential of salivary acinar cells or on their ability to generate overshooting action potentials when stimulated electrically, although prolonged vanadate exposure decreased the safety factor for synaptic transmission. Decreased synaptic efficacy was not observed after the relatively brief (5 min) exposure periods used in the experiments described below.

Generation of Action Potentials in Acinar and Central Duct Cells

The *Helisoma* salivary gland can be divided into three morphologically distinct regions: the anterior duct, the central duct, and the secretory acini (Fig. 2). The most proximal region of the gland, the anterior duct, channels the saliva into the buccal cavity. It is distinguished from the central duct region by its lack of acinar outpocketings or diverticula. Commonly, the acinar diverticula are arranged bilaterally along either side of the central duct. In contrast with many gastropod salivary glands, interlobular ducts appear to be absent, the lumen of each acinus communicating directly with the lumen of the central duct.

Previous investigations of the snail salivary gland have been limited to intracellular recordings from acinar cells; the electrical behavior of cells forming the central and anterior ducts has not been reported. The electrophysiological characterization of central duct cells is of particular interest because membrane currents generated in one acinus must be conducted through these cells in order to affect neighboring acini, particularly acini that are situated laterally across the central duct.

To compare the responses of acinar and central duct cells to neural stimulation, we carried out a series of experiments in which the images of acinar and central duct regions were focused onto different regions of a 5 × 5 photodiode array. The results of a typical experiment are shown in Fig. 2. The gland region monitored by each photodetector element is indicated on the perspective drawing of the preparation. (For this experiment, only 15 of the 25 photodiode elements were used.) Gland stimulation was provided by a brief shock to the salivary nerve through a suction electrode, and the electrical responses recorded optically are displayed at the locations corresponding to the gland regions from which they were obtained.

All detectors recorded a gland action potential in response to stimulation of the salivary nerve. The waveform of action potentials recorded by the detectors positioned over the central duct (middle row) is similar to that observed for action potentials generated by acinar gland regions. (Differences in response amplitude have no direct physiological significance, because the magnitude of the optical signal depends upon a number of factors, including the membrane area and amount of dye bound, that cannot be readily assessed.) This suggests

that all or at least a substantial fraction of the cells forming the central duct respond to neural stimulation with a regenerative action potential similar in waveform and duration to that observed in secretory acinar cells. This result was subsequently confirmed using conventional intracellular recording techniques.

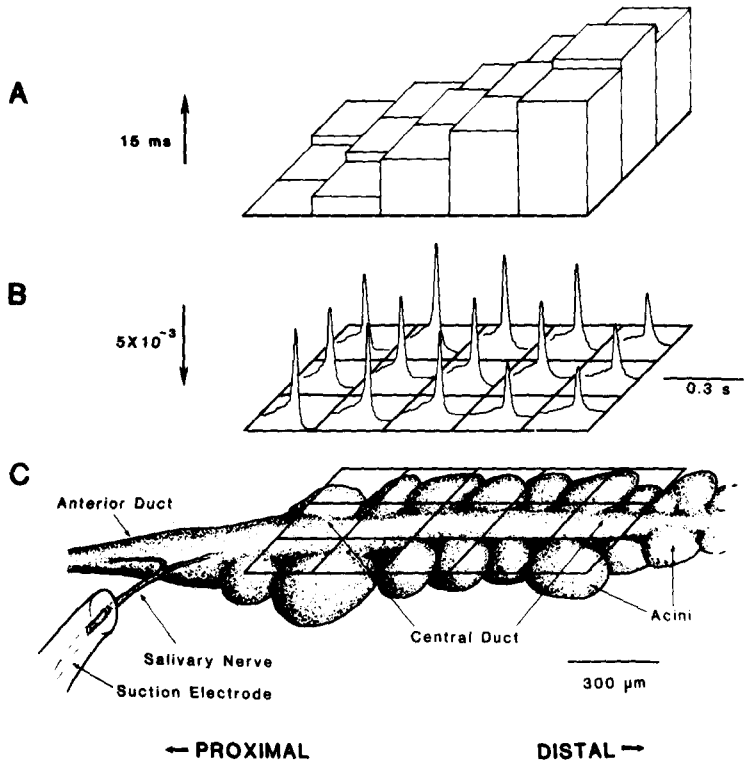

FIGURE 2. Lateral synchrony of neurally evoked action potentials recorded optically from contiguous acinar and central duct regions. Part A: the vertical height above each array element is proportional to the time-to-peak of the action potential recorded from the corresponding gland region, relative to the first peak recorded by the lower left array element. Differences in times-to-peak are more pronounced in the longitudinal direction than in the transverse direction. Part B: optical recordings of gland responses are displayed superimposed upon the detector elements from which they were recorded. Single trial. Part C: the approximate gland regions monitored by each array element are indicated. The middle row of detectors monitored the central duct; the two lateral rows monitored acinar diverticula. A suction electrode on the salivary nerve was used for stimulation.

Synchronized Activity in Laterally Opposed Acini

Previous investigations have shown that the coupling between cells within a single acinus was significantly higher than that observed between cells in adjacent acini (Kater et al. 1978*a*; Bahls et al., 1980), which suggests the

possibility of independent propagation on either side of the central duct. However, the generation of action potentials by central duct cells ensures synchrony of activity between laterally opposed acini. The degree of lateral synchronization is revealed by the histogram at the top of Fig. 2. Here, the vertical height above each element is proportional to the time to peak of the action potential. (Times to peak were plotted as delays from the earliest peak response recorded by the element at the extreme lower left.) The peak of the regenerative response is nearly simultaneous in laterally opposed acini and in the interposed central duct region, as the action potential sweeps distally down the gland. This result was typical; the wavefront advanced symmetrically along laterally opposed acini. No examples were found in which propagation was restricted to the central duct or to acini on one side or the other of the gland.

Lateral synchrony was observed also in cases in which neural stimulation evoked a complex, multiphasic response in the gland. This is illustrated in Fig. 3. As in the previous record (Fig. 2), the gland was stimulated with a

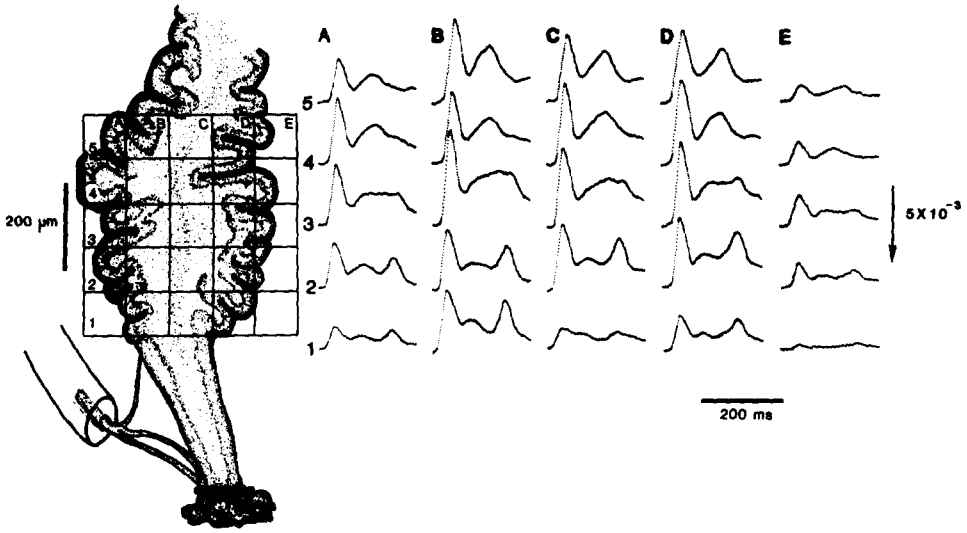

FIGURE 3. Lateral synchrony of complex gland potentials in contiguous gland regions. A single brief shock to the salivary nerve evokes a complex multiphasic gland response. The first component is an action potential which is followed by a second component that shows regional variation in waveform. The waveform of the second component exhibits less variation between laterally contiguous gland regions than longitudinally contiguous regions, which suggests a higher degree of electrical coupling along the transverse gland axis. The optical responses recorded by the elements in row E (E-1–E-5) and by element A-1 were markedly degraded and were not used for comparison. Signal-to-noise attenuation in these array elements resulted from partial tissue coverage and consequently large background light levels monitored by these array elements. The response obtained by element C-1 was also omitted from the comparison. This element almost exclusively monitored epithelial cells in the anterior duct that do not show regenerative membrane potential changes in response to neural stimulation (cf. Fig. 5).

single, brief shock to the salivary gland nerve. In this instance, however, the optically recorded gland action potential is followed by a secondary response of variable waveform. (Complex gland responses are frequently observed in healthy, unstained preparations. This complexity may reflect the connectivity of the tissue, ionic mechanisms, or both.)

If the secondary components of the gland response are compared element by element (excluding elements in column E and elements A-1 and C-1; see the legend to Fig. 3), the variation in the optical waveform is more marked in the longitudinal than in the transverse direction, which suggests that electrical coupling is tighter across the gland than down its length. (The extent to which these differences reflect differences in the effective length constant for lateral and longitudinal current spread has not yet been determined.)

Longitudinal Delay in EPSP Onset

The initial electrical event following stimulation of the salivary gland nerve is a transient depolarization of acinar cells by several millivolts. Sometimes, but not always, this depolarization elicits an action potential at the recording site (Kater et al., 1978*b*; Bahls et al., 1980). It has been suggested by these authors that this initial depolarization represents a chemically mediated EPSP. However, it is not possible on the evidence of amplitude and waveform alone to distinguish between a chemically mediated EPSP and an electrotonic reflection of a gland action potential initiated at some remote site (e.g., see Fig. 5 in Kater et al., 1978*b*).

If the initial depolarization of acinar and/or central duct cells after neuronal stimulation is affected by a chemically mediated EPSP, then the foot of the depolarization should be progressively retarded along the longitudinal gland axis as a result of the conduction delay of the nerve impulse in the presynaptic nerve fibers. Using conventional electrophysiological methods, we measured the conduction velocity of the SEN impulse to be ~0.11 m/s (Fig. 4). At this relatively slow conduction velocity, an appreciable distance-dependent delay in the rise of the optical response is anticipated. For a presynaptic impulse having a conduction velocity of 0.11 m/s, the expected foot of the EPSP is indicated graphically by the interrupted line in Fig. 4. The filled triangles show the delay in response onset from one experiment in which an intracellular microelectrode was used to drive the contralateral SEN. To improve the signal-to-noise ratio of the optical response, the results of 10 trials were averaged. At the stimulation rate used (0.5 Hz), the gland action potential failed to follow the neuron spike although a transient depolarization was recorded by each array element. The 15 array elements used in this experiment covered ~90% of the gland, excluding the anterior duct.

The solid line represents the best fit to the data determined by a linear regression ($r = +0.82$). The slope (1.61 elements/ms) is equivalent to a progressive longitudinal delay in the response onset of 8.33 ms/mm. This corresponds to a velocity of 0.12 m/s, which agrees well with the experimentally derived conduction velocity for the SEN nerve impulse (0.11 m/s). Comparable results were also obtained in single trials in which neuronal stimulation evoked a gland action potential (e.g., Fig. 5 below), although data

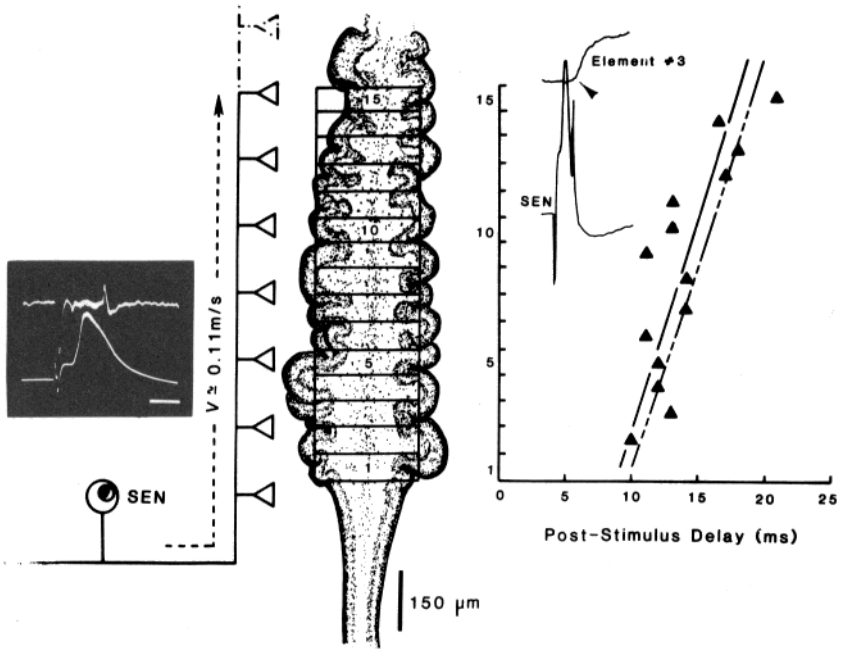

FIGURE 4. Transit time of the presynaptic SEN nerve spike accounts for the longitudinal delay in the onset of the gland EPSP. Data used to calculate the conduction velocity of the SEN nerve impulse are shown in the inset at the left of the figure. The lower trace of the inset shows an action potential in the ipsilateral SEN evoked by intracellular current injection; the upper trace shows the propagating nerve impulse recorded in the salivary nerve with a suction electrode. The calibration bar is 5 ms; the distance between the SEN cell body and the nerve recording site was 715 μm, yielding a conduction velocity of 0.11 m/s. The drawing of the preparation shows the gland regions monitored by each of the 15 elements of the linear array used in this experiment. The graph shows the data used to measure the post-stimulus delay in the onset of the EPSP. The lower record on the graph shows the action potential in a contralateral SEN evoked by intracellular current injection; the upper record shows the gland EPSP recorded optically by array element 3. The results of 10 trials were averaged to improve the signal-to-noise ratio of the optical recordings. The delay between the peak of the SEN action potential and the foot of the EPSP (at arrow) is plotted on the abscissa; the ordinate represents the array element number and hence longitudinal displacement along the gland. The filled triangles show the delays in the onset of the EPSP in each gland region, determined optically. The solid line is the least-squares linear fit to the data. The interrupted line is the expected delay in EPSP onset calculated from the conduction velocity of the SEN nerve impulse. See text for additional details.

from these experiments exhibited more scatter as a result of the decreased signal-to-noise ratio in the optical records, and the regression analyses indicated somewhat lower conduction velocities. S. B. Kater and A. D. Murphy (personal communication) have show, by means of intracellular injection of Lucifer yellow CH, that there is a significant reduction in the diameter of the

SEN axons as they course over the gland. Thus, a slower conduction velocity would be expected in the innervating fibers, compared with the nerve trunk on which the measurements were carried out.

Since the longitudinal delay in response onset can be explained by the transit time of the presynaptic nerve impulse along the gland, it is most reasonable to assume that the transient depolarization of gland cells after neuronal stimulation is predominantly, if not exclusively, the result of a chemically mediated EPSP, as suggested previously by Kater et al. (1978*b*). An important consequence is that all gland regions (excluding the anterior duct) receive excitatory synaptic input. This follows from the fact that the onset of response in all gland regions is well described by a single linear-regression line.

Activation of Gland Action Potentials

Neuronal stimulation of the gland could activate the regenerative response in two distinguishable ways. If the level of depolarization generated by the EPSP were relatively high, activation of the regenerative response might occur in all gland regions directly. However, if the depolarization produced by the EPSP were relatively low, activation of the regenerative response might occur only in a relatively restricted, and perhaps specialized, gland region. This action potential would provide an additional source of depolarizing current, augmenting the effect of the EPSP through electrotonic spread. Most of the experiments are readily explained by assuming that both processes are involved in gland activation. In some gland regions, the EPSP appeared to activate the regenerative response directly, while at other sites, activation followed electrotonic spread. Fig. 5 shows the results of a typical experiment in which both processes contributed to the complete activation of the gland.

The relative contribution of each process to the activation of a given gland region can be deduced from the interval between the onset of the EPSP and the peak of the regenerative response. At the right of Fig. 5, the times of response onset (filled circles) and action potential peak (open circles) recorded from each gland region have been plotted as the delay from the spike in the contralateral SEN. As in the previous figure, the onset of depolarization was retarded as a function of distance along the longitudinal gland axis. The linear-regression line for the onset data (solid line) has a slope value of 1.03 elements/ms, corresponding to a longitudinal velocity of 0.07 m/s. The dotted line is drawn parallel to the regression line at an interval equal to the delay between the response onset and the peak of the first action potential to occur after stimulation. We assume that the gland region displaying the earliest peak response, in this instance the region monitored by element 4 (filled square), was directly activated by the EPSP. If we assume further that the kinetics of direct synaptic activation are relatively independent of gland location, a similar interval between response onset and action potential peak would be expected in other gland regions in which activation was primarily affected by the EPSP. On these assumptions, direct synaptic activation appears to have occurred in proximal regions of the gland (array elements 4–12), but not at more distal sites where the peaks of the regenerative response

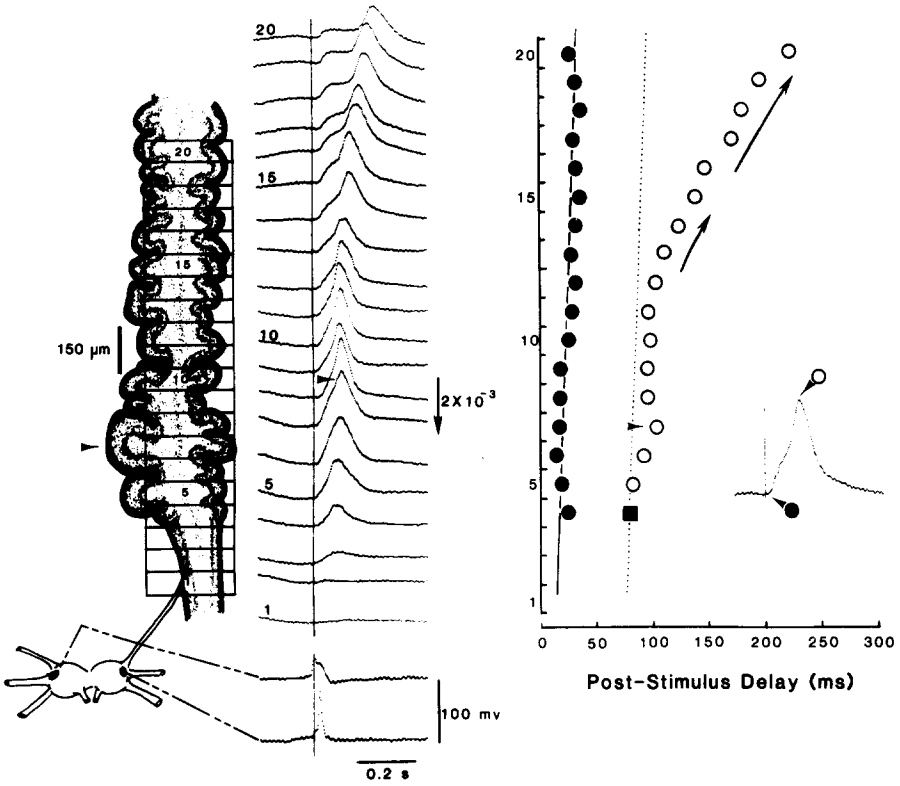

FIGURE 5. Typical pattern of gland activation resulting from neuronal stimulation. The drawing of the preparation shows the gland regions monitored by each of the 20 array elements. The electrical activity in both SENs was monitored with intracellular microelectrodes. The vertical line drawn through the optical recordings of the responses marks the time of the action potential peak in the contralateral SEN. The optical record inset on the graph shows the response recorded by array element 8 to illustrate the two response parameters plotted: the onset of response (filled circles) and the peak response (open circles). The earliest peak response recorded is shown by the filled square. The onset time and time-to-peak recorded by each array element are plotted on the abscissa as delays from the peak of the SEN action potential. The ordinate represents the longitudinal distance along the gland in terms of the array element numbers. The solid line is the linear least-squares fit for the onset data. The dotted line was drawn through the earliest peak response and parallel to the best fit of the data to define the minimum interval for activation of the regenerative response. Arrows indicate the direction and approximate velocity of the electrotonically conducted gland action potential. The pointers indicate an extraordinarily large acinus and the anomalous peak response associated with the same gland region. See text for additional details.

fall substantially beyond this minimum interval. Activation of these distal gland regions thus results primarily from the action potential conducted electrotonically from more proximal areas of the gland.

Velocity of Excitation Spread

The data in Fig. 5 have been plotted as a distance (i.e., element number) as a function of time (i.e., response delay). The instantaneous velocity of excitation spread in the gland, therefore, is directly related to the slope of the line connecting adjacent data points. In the proximal gland regions directly activated by the EPSP, the longitudinal delay in the peak of the action potential does not indicate excitation spread in the gland per se, but rather reflects the transit time of the presynaptic nerve impulse. The response recorded by element 7 (indicated by the arrow) appears anomalously retarded, since the action potential peak in this region occurred after those in more distal regions. We believe this delay is a consequence of the unusually large acinus in this gland region (at arrow), with its additional capacitative load slowing the rate of depolarization by the EPSP and delaying the activation process locally.

The velocity of excitation spread in the distal half of the gland was ~5 mm/s or 14 times slower than the conduction velocity of the neural spike. We believe that this slow velocity reflects the interaction between two factors, the level of depolarization required to activate the regenerative response and the capacitative load imposed on the distally spreading electrotonic current. Because the membrane area in each distal gland region is quite large, it is reasonable to assume that effects of capacitative loading will be correspondingly large and will severely limit the velocity of excitation spread.

Variability of Activation Patterns

In most experimental trials, neural stimulation of the gland was found to activate the proximal gland region directly, whereas activation in more distal gland regions resulted from the electrotonically propagated action potential as shown in Fig. 5. Occasionally, different patterns of activation were observed. This variability in the pattern of activation is summarized in Table I. Fig. 6 shows the results of three trials obtained from a single preparation that exhibited considerable variability in the pattern of activation. Measurements of the time to peak of the regenerative response recorded at each site have been plotted in Fig. 7. In trial 1, the first recorded action potential occurred in a distal gland region (filled square). Action potentials spread distally and proximally from this point. The velocity of the action potential conducted in a proximal direction decreased as a function of distances from the site of initiation.

In trial 2, the first action potential evoked by nerve stimulation occurred in the typical proximal gland region (solid square), initiating an action potential that propagated in a distal gland direction. Approximately 11 ms after this action potential was initiated, a second action potential arose in a more distal gland region. This action potential was propagated electrotonically distally

and proximally. The filled circle indicates the approximate gland region in which the converging action potentials collide. Because gland cells between the converging action potentials are electrotonically depolarized by both advancing excitatory waves, the velocity of excitatory spread dramatically increases before the moment of collision. This rapid increase in the velocity of propagation of colliding action potentials was even more apparent in trial 3. Here, a proximally directed action potential was first initiated at a distal gland locus; after a 4-ms delay, a distally propagated action potential was

TABLE I

DIRECTION OF ELECTROTONICALLY PROPAGATED ACTION POTENTIALS IN SNAIL GLAND PREPARATION

Preparation	Distal	Proximal	Trials
1	0	5	5
2	1	1	2
3	1	2	3
4	2	0	2
5	1	2	3
6	7	0	7
7	7	0	7
8	2	0	2
9	3	1	4
10	5	0	5
11	5	0	5
12	1	1	2
13	1	0	1
14	4	0	4
15	4	2	6
16	10	0	10
17	8	0	8
18	3	1	4
19	3	7	10
Total:	68	22	90
Percent of total trials:	76%	24%	100%

initiated. The velocities of these electrotonically propagated action potentials increase just before their collision in the gland region indicated by the filled circle.

DISCUSSION

Cellular Origin of the Optical Signal

The salivary gland of the snail *Helisoma* is composed of several morphologically and/or functionally distinct cell types. The most comprehensive histological study of the basommatophoran salivary gland has been made by Boer et al. (1967) in a species closely related to *Helisoma*, *Lymnaea stagnalis*. These authors recognized 10 different cell types, including 7 types of secretory cells (granular cells, pseudochromosome cells, mucocytes I and II, cells with acidophilic

inclusions, grain cells, mixed cells), precursors of secretory cells (basophilic cells), ciliated cells, and squamous epithelial cells. Because a number of different cell types may occur in any given gland region, the cellular basis of the optically recorded membrane signal is less certain in the gland than in

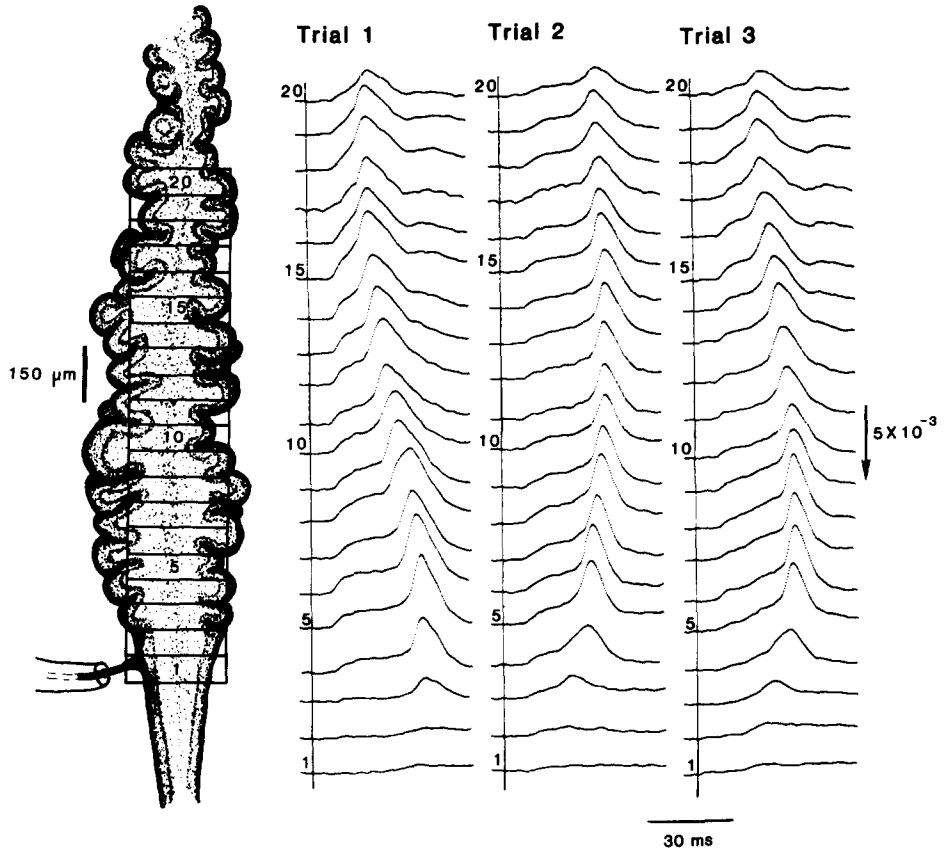

FIGURE 6. Intertrial variability of gland activation pattern. The drawing shows the gland regions monitored by each of the 20 array elements. Optically recorded responses evoked by nerve stimulation are shown for three consecutive trials. The vertical line drawn through the optical signals marks the onset of nerve stimulation. See text for additional details.

other tissues studied previously by this technique (Cohen and Salzberg, 1978; Salzberg, 1983).

The gland area, and hence the number of cells monitored by each element in the photodiode array, depended upon the magnification of the microscope objective. Even at the highest power used (× 20), the light detected by a single array element may be estimated conservatively to have traversed a region of salivary gland containing between several hundred and a few thousand cells. Membrane potential changes in each cell would contribute to the recorded

change in light absorption as a function of the cell's absolute change in membrane potential, the total area and orientation of the cell's membrane in the optical path, the total amount of dye bound to its membrane, and the relative amount of dye bound to inexcitable membrane. The concentration of dye bound to each cell would depend upon the dye's access to the luminal and extraluminal cell surfaces as well as its binding affinity with the cell's membrane. Although we have no evidence to suggest that the binding affinity

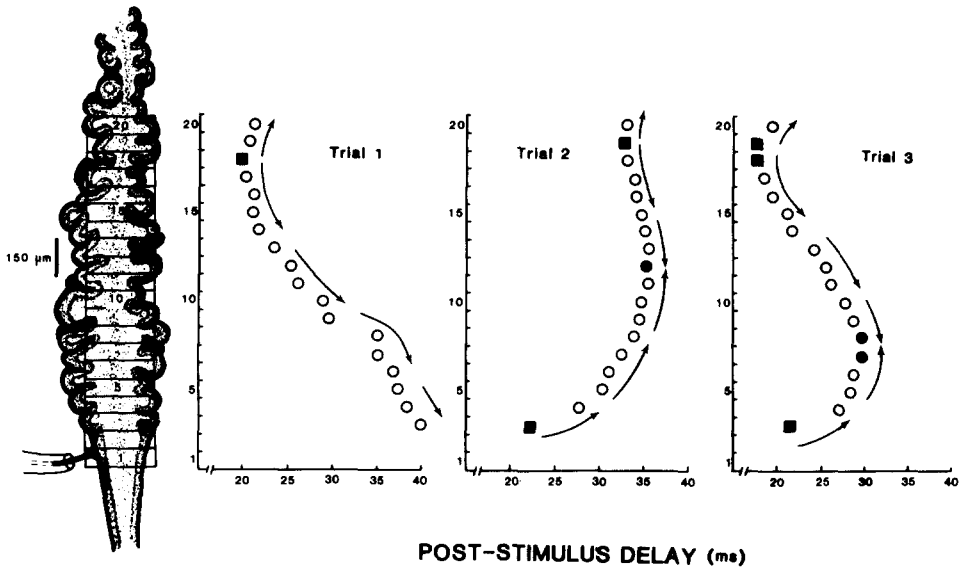

FIGURE 7. Graphic representation of the optical data shown in Fig. 6. The delay between nerve stimulation and the peak of the gland action potential (open circles) has been plotted as a function of gland location. The ordinate represents longitudinal displacement along the gland plotted as array element number. The solid squares indicate the gland loci at which propagating gland action potentials were initiated. The arrows indicate the direction and approximate velocity of the propagating action potentials. The filled circles indicate the gland regions at which converging gland action potentials collide. See text for additional details.

of the merocyanine-oxazolone dye used (NK 2367) varies among gland cell types, the possibility that certain cell types were selectively stained and hence are unequally represented in the optical signals cannot be ruled out (e.g., see Salzberg et al., 1982).

On the simplest assumption, the optical signals obtained in these experiments represent a weighted average of the membrane potential changes in at least a few, if not all, gland cell types. It should be emphasized that although the optical signals are multicellular in origin, they are directly related to the transmembrane potential changes in the cells in the light path and not to the existence of extracellular "field potentials." Based on differences in relative size, number, and regional distribution of the various cell types, together with

the results of conventional intracellular microelectrode recordings from various gland regions, the cell types most likely to be responsible for the recorded optical signals can be deduced. Light and electron microscopic studies of the *Helisoma* salivary gland (D. Senseman and P. Orkand, unpublished data) have shown that the largest and most numerous cell types composing the acinar diverticula are analogous to mucocytes I and II of Boer et al. (1967). It is very likely, therefore, that most of the intracellular recordings from acinar regions are from these cell types. Because there is a close correspondence between intracellular recordings and optical recordings from the same acinus (Fig. 1), the optical signals generated in the acinar regions are probably dominated by mucocyte I and II activity. Similarly, the optical signals recorded from the central duct region are probably dominated by electrical activity in granular cells, which are believed to release the secretory enzyme amylase (Boer et al., 1967), and pseudochromosome cells, whose secretory function is still unclear.

Our failure to detect an optical signal from the membrane comprising the anterior duct after neuronal stimulation (Figs. 5 and 6) is not unexpected, because this region is composed predominantly of nonsecretory cells (squamous epithelial) that do not exhibit regenerative electrical activity. Of the remaining cell types, only the ciliated cell occurs in significant numbers. The comparatively small size and slender shape (1–2 μm wide) of these cells has discouraged intracellular microelectrode recordings and no reports of successful penetrations of ciliated cells have appeared. Although the metachronous beating of cilia increased the optical noise manyfold, the contribution of possible membrane potential changes in ciliated cells to the optical signal is not known. We did not observe any significant change in the amplitude or waveform of the optical signal when ciliary motility in these cells was inhibited with sodium metavanadate. As yet, we do not know whether these cells are electrically active and/or coupled to other cell types, or whether vanadate treatment alters their electrical properties in addition to its inhibition of the dynein ATPase.

Synaptic Activation

The results presented here support and extend the basic conclusions reached by Kater and his co-workers (Kater et al., 1978*a*, *b*; Bahls et al., 1980) concerning the activation of the regenerative gland response by neuronal stimulation. All gland regions appear to receive direct excitatory synaptic input from the SENs because neuronal stimulation evoked a transient depolarization (EPSP) in both proximal and distal gland regions (Figs. 5 and 6) and the delay in the response onset could be explained by the conduction delay of the SEN nerve impulse (Fig. 4). However, within a given gland region, the number of cells receiving a direct synaptic input compared with the number of adjacent coupled cells depolarized electrotonically by the EPSP is unknown. Axons from both SENs are present in each salivary nerve and both neurons were found to innervate each salivary gland. Whether the synaptic fields of the two SENs overlap has not been determined, although we have observed significant differences in the pattern of gland activation when SENs are singly or synchronously stimulated (unpublished observations). No

evidence was found to suggest the involvement of a peripheral neuron network in the activation of the gland by the SENs.

The pattern of gland activation evoked by neural stimulation showed considerable variability from preparation to preparation and between successive trials in the same preparation (Table I). Most frequently, the EPSP was large enough to activate a regenerative response in the proximal region of the central duct, where the most proximal segment, at the point of its confluence with the anterior duct, reached its peak depolarization before other gland regions. This circumstance probably results from two factors. Certainly, the presynaptic nerve spike reaches the synaptic terminals in the proximal region of the central duct before more distal gland regions (Fig. 4). Less obvious is the fact that, in contrast with other gland regions, the proximal portion of the central duct is juxtaposed with the anterior duct. Because cells in the anterior duct do not depolarize significantly when adjacent central duct cells are synaptically activated (Fig. 5), electrotonic coupling between these regions might be low. If this were true, the anterior duct would not serve as a large current sink. Consequently, the effective input impedance of the proximal part of the central duct would be greater than that of other gland regions and the EPSP would be more effective in activating the regenerative response. Direct measurements of coupling efficacy between central and anterior duct cells will be necessary, however, to substantiate (or refute) this hypothesis.

The relative size of different gland regions also appeared to alter the pattern of activation. Complete activation of gland regions containing extraordinarily large acini was frequently delayed slightly, compared with neighboring sites (e.g., Fig. 5). Conversely, gland regions with relatively small acinar diverticula occasionally achieved complete activation before adjacent loci. In such cases, the action potential generated was usually propagated in both proximal and distal directions (e.g., Fig. 6). We believe that the effects of regional differences in gland mass on the pattern of activation can be explained in terms of the corresponding differences in capacitative load imposed on synaptic and electrotonic currents. Larger acinar outpocketings contain more cells, and this increased capacitative load would slow the rate of depolarization produced by either synaptic or electrotonic currents, delaying the region's complete activation. In smaller gland regions, the reduced load would accelerate activation.

Electrotonic Propagation of Action Potentials

The ability of an action potential initiated at one gland locus to propagate electrotonically from the site of initiation was first demonstrated by Kater et al. (1978*a*). The results presented here suggest further that such electrotonic propagation is important physiologically to ensure complete activation of the gland after neuronal stimulation. In only one of the more than 100 trials that we performed did we observe complete activation of the gland by the EPSP. In all other trials, only a portion of the gland (usually the proximal region of the central duct and its acinar outpocketings) was activated directly by the EPSP, with activation of the remainder of the gland mediated by the electrotonic propagation of the evoked action potential. Under the conditions

imposed by the experimental arrangement, electrotonic propagation of the regenerative response appears to act in an auxiliary fashion with direct synaptic activation. Gland regions in which the EPSP fails to activate the regenerative response are subsequently invaded by a propagated action potential.

Implications of Possible Pharmacological Effects

An important question is the extent to which the pattern of activation was modified by the experimental conditions. Treatment of the gland with $NaVO_3$ to inhibit ciliary motility may have caused some reduction in synaptic efficacy, even with the relatively brief exposure periods used. If so, the physiological significance of electrotonic activation would be exaggerated. In a few experiments we eliminated the $NaVO_3$ treatment in order to assess its possible pharmacological effects. These attempts were not entirely successful because of the high level of optical noise introduced by the beating cilia. However, the results did suggest that the basic pattern of gland activation was not materially affected by brief exposures to 10 mM $NaVO_3$.

We were somewhat more concerned with the pharmacological effects of NK 2367, the potentiometric probe itself. These effects can be separated into light-dependent and light-independent parts. Serious light-independent pharmacodynamic changes were observed when glands were stained for 20 min with concentrations of NK 2367 of ≥ 0.05 mg/ml if the dye was dissolved in normal snail Ringer's solution. Action potentials were observed in which the upstroke velocity was fairly normal but which exhibited an abnormally prolonged recovery phase (>500 ms). This effect occurred in the absence of strong illumination. We discovered that this light-independent dye intoxication could be virtually eliminated by raising the divalent cation concentration of the staining solution. Although the mechanism of this "protection" is unclear, higher dye concentrations were observed to yield larger optical signals, which suggests that the elevated divalent cation concentration did not act by inhibiting probe binding to the membrane. A plausible explanation is that during staining, when the equilibrium concentration of the probe in the membrane is maximal, some portion of the negative surface charge contributed by the sulfonate moiety is effectively screened by the divalents.

During the course of an experiment, we frequently observed a gradual broadening of the gland action potential. This effect was light dependent and presumably resulted from photodynamic damage (Pooler, 1972; Cohen and Salzberg, 1978; Salzberg, 1983). As a result, the initial trials in a given experiment were considered to be more reliable and were accorded greater significance in the data analysis.

Utility of Multiple-Site Optical Recording

As Loewenstein (1981) has pointed out, the tenets incorporated in classic cell theory are clearly inadequate when applied to organized tissues in which there exists a high degree of electrical coupling: "It is the coupled cell ensemble, and not the single cell, that is the functional compartmental unit. . . ." Weid-

mann (1952) was the first to recognize that tissues (such as cardiac muscle) can be organized as electrical syncytia, and that such tissues may exhibit complex electrical properties. The behavior of such syncytia differs in unique and unexpected ways from the electrical behavior observed in single cells with conventional microelectrodes. The recognition and study of such emergent tissue properties requires the simultaneous assessment of potential changes in many, if not all, tissue regions. The results presented above for a simple gland, as well as analogous studies in heart (Dillon and Morad, 1981; Fujii et al., 1981) clearly demonstrate the utility of multiple-site optical recording of membrane potential for the investigation of electrical syncytia. Other electrically active syncytia, e.g., tadpole skin (Roberts and Stirling, 1971) and the *rete mirabile* of coelenterates (Mackie, 1976) should also be amenable to investigation by this approach.

The most obvious "global" property of snail salivary glands to emerge in the present study is the relatively high degree of lateral synchronization of electrical activity compared with the relatively slow propagation observed along the longitudinal gland axis. This anisotrophy of electrical excitation in the gland is reminiscent of the situation in cardiac tissue (Woodbury and Crill, 1961) but has not previously been reported in an exocrine or endocrine system. Using intracellularly injected current pulses in conjunction with multiple-site optical recording techniques, it should be possible to ascertain whether anisotropic excitation is a direct consequence of anisotropic electrical coupling between acinar and central duct cells. To provide increased spatial resolution for this and other experiments, we have recently expanded our data acquisition system to monitor optical changes from 124 sites simultaneously.

Supported by U.S. Public Health Service grants DE 05271 and NS 16824.
We are most grateful to Larry Cohen and Sarah Lesher for generously providing the software used for the acquisition and display of the optical signals. We would also like to thank Drs. Larry Cohen, Stan Kater, and Don Murphy for their critical reading of the manuscript.

Received for publication 13 January 1983 and in revised form 7 March 1983.

REFERENCES

Bahls, F., S. B. Kater, and R. W. Joyner. 1980. Neuronal mechanisms for bilateral coordination of salivary gland activity in *Helisoma*. *J. Neurobiol.* 11:365–379.

Boer, H. H., S. E. Wendelaar Bonga, and N. van Rooyen. 1967. Light and electron microscopical investigations on the salivary glands of *Lymnaea stagnalis* L. *Z. Zellforsch. Mikrosk. Anat.* 76:228–247.

Cohen, L. B., and B. M. Salzberg. 1978. Optical measurement of membrane potential. *Rev. Physiol. Biochem. Pharmacol.* 83:35–88.

Dillon, S., and M. Morad. 1981. A new laser scanning system for measuring action potential propagation in the heart. *Science* (*Wash. DC*). 214:453–455.

Fujii, S., A. Hirota, and K. Kamino. 1981. Action potential synchrony in embryonic precontractile chick heart: optical monitoring with potentiometric dyes. *J. Physiol.* (*Lond.*). 319:529–541.

Gibbons, I. R., M. P. Losson, J. A. Evans, B. H. Gibbons, B. Houck, K. H. Martinson, W. S. Sale, and W.-J. X. Tang. 1978. Potent inhibition of dynein adenosinetriphosphatase and of motility of cilia and sperm flagella by vanadate. *Proc. Natl. Acad. Sci. USA.* 75:2220–2224.

Ginsborg, B. L., C. R. House, and E. M. Silinsky. 1974. Conductance changes associated with the secretory potential in the cockroach salivary gland. *J. Physiol. (Lond.).* 236:723–737.

Grinvald, A., L. B. Cohen, S. Lesher, and M. B. Boyle. 1981. Simultaneous optical monitoring of activity of many neurons in invertebrate ganglia using a 124-element photodiode array. *J. Neurophysiol.* 45:829–840.

Iwatsuki, N., and O. H. Petersen. 1978*a*. Membrane potential, resistance and intercellular communication in the lacrimal gland: effects of acetylcholine and adrenaline. *J. Physiol. (Lond.).* 275:507–520.

Iwatsuki, N., and O. H. Petersen. 1978*b*. Electrical coupling and uncoupling of exocrine acinar cells. *J. Cell Biol.* 79:533–545.

Kagayama, M., and A. Nishiyama. 1974. Membrane potential and input resistance in acinar cells from cat and rabbit submaxillary glands in vivo: effects of autonomic nerve stimulation. *J. Physiol. (Lond.).* 242:157–172.

Kater, S. B., and N. J. Galvin. 1978. Physiological and morphological evidence for coupling in mouse salivary gland acinar cells. *J. Cell Biol.* 79:20–26.

Kater, S. B., J. R. Rued, and A. D. Murphy. 1978*a*. Propagation of action potentials through electrotonic junctions in the salivary glands of the pulmonate mollusc, *Helisoma trivolvis. J. Exp. Biol.* 72:77–90.

Kater, S. B., A. D. Murphy, and J. R. Rued. 1978*b*. Control of the salivary glands of *Helisoma* by identified neurones. *J. Exp. Biol.* 72:91–106.

Křivánek, J. 1981. In vivo electrical stimulation alters sensitivity of the brain ($Na^+ + K^+$) ATPase toward inhibition by vanadate. *J. Neurobiol.* 12:343–352.

Loewenstein, W. R. 1981. Junctional intercellular communication: the cell-to-cell membrane channel. *Physiol. Rev.* 61:829–913.

Lundberg, A. 1955. The electrophysiology of the submaxillary gland of the cat. *Acta Physiol. Scand.* 35:1–25.

Mackie, G. O. 1976. Propagated spikes and secretion in a coelenterate glandular epithelium. *J. Gen. Physiol.* 68:313–325.

Petersen, O. H. 1980. The Electrophysiology of Gland Cells. Academic Press, Inc., New York. 36–64.

Petersen, O. H., and N. Ueda. 1976. Pancreatic acinar cells: the role of calcium in stimulus-secretion coupling. *J. Physiol. (Lond.).* 254:583–606.

Pooler, J. 1972. Photodynamic alteration of sodium currents in lobster axons. *J. Gen. Physiol.* 60:367–387.

Roberts, A., and C. A. Stirling. 1971. The properties and propagation of a cardiac-like impulse in the skin of young tadpoles. *Z. Vgl. Physiol.* 71:295–310.

Roberts, M. L., N. Iwatsuki, and O. H. Petersen. 1978. Parotid acinar cells: ionic dependence of acetylcholine-evoked membrane potential changes. *Pflügers Arch. Eur. J. Physiol.* 376:159–167.

Salama, G., D. M. Senseman, I. S. Horwitz, and B. M. Salzberg. 1980. Vanadate inhibits ciliary beating in intact snail salivary glands. *Biol. Bull. (Woods Hole).* 159:444–445.

Salzberg, B. M. 1983. Optical recording of electrical activity in neurons using molecular probes. *In* Current Methods in Cellular Neurobiology. J. Barker and J. McKelvy, editors. John Wiley & Sons, Inc., New York. In press.

Salzberg, B. M., and D. M. Senseman. 1979. Optical spikes from a salivary gland. *Soc. Neurosci. Abstr.* 5:260. (Abstr.)

Salzberg, B. M., A. Grinvald, L. B. Cohen, H. V. Davila, and W. N. Ross. 1977. Optical recording of neuronal activity in an invertebrate central nervous system: simultaneous monitoring of several neurons. *J. Neurophysiol.* 40:1281–1291.

Salzberg, B. M., A. L. Obaid, H. Shimizu, R. K. Orkand, and D. M. Senseman. 1982. Does the Schwann cell of *Loligo* act as a potassium electrode? *Biol. Bull. (Woods Hole).* 163:390.

Salzberg, B. M., D. M. Senseman, and G. Salama. 1981. Multiple site optical recording of membrane potential from an electrical syncytium: monitoring the spread of excitation in a salivary gland. *Biophys. J.* 33:90*a*. (Abstr.)

Senseman, D. M., and B. M. Salzberg. 1980. Electrical activity in an exocrine gland: optical recording with a potentiometric dye. *Science (Wash. DC).* 208:1269–1271.

Simpson, I., B. Rose, and W. R. Loewenstein. 1977. Size limit of molecules permeating the junctional membrane channels. *Science (Wash. DC).* 195:294–296.

Waggoner, A. 1979. Dye indicators of membrane potential. *Annu. Rev. Biophys. Bioeng.* 8:47–63.

Weidmann, S. 1952. The electrical constants of Purkinje fibres. *J. Physiol. (Lond.).* 118:348–360.

Westenfelder, C., R. K. Hamburger, and M. E. Garcia. 1981. Effects of vanadate on renal tubular function in rats. *Am. J. Physiol.* 240:F522–F529.

Woodbury, J. W., and W. E. Crill. 1961. On the problem of impulse conduction in the atrium. *In* Nervous Inhibition. E. Florey, editor. Pergamon Press, Oxford. 124–135.

Young, J. A., and E. W. van Lennep. 1978. The Morphology of Salivary Glands. Academic Press, Inc., New York. 102–103.